

1 **SEALDH-II – a calibration-free transfer standard for airborne water vapor measurements:**
2 **Pressure dependent absolute validation from 5 – 1200 ppmv**
3 **at a metrological humidity generator**

4
5 **Bernhard Buchholz^{1,2,4}, Volker Ebert^{1,2,3}**

6 ¹ *Physikalisch-Technische Bundesanstalt Braunschweig, Germany*

7 ² *Physikalisch Chemisches Institut, Universität Heidelberg, Germany*

8 ³ *Center of Smart Interfaces, Technische Universität Darmstadt, Germany*

9 ⁴*currently at Department of Civil and Environmental Engineering, Princeton University, USA.*

10 *Corresponding author: volker.ebert@ptb.de*

11
12
13 **Abstract**

14 Highly accurate water vapor measurements are indispensable for understanding a variety of scientific
15 questions as well as industrial processes. While in metrology water vapor concentrations can be defined,
16 generated and measured with relative uncertainties in the single percentage range, field deployable
17 airborne instruments deviate even under quasi-static laboratory conditions up to 10-20%. The novel
18 SEALDH-II hygrometer, a calibration-free, tuneable diode laser spectrometer, bridges this gap by
19 implementing a new holistic concept to achieve higher accuracy levels in the field. Here we present the
20 absolute validation of SEALDH-II at a traceable humidity generator during 23 days of permanent operation
21 at 15 different H₂O concentration levels between 5 and 1200 ppmv. At each concentration level, we studied
22 the pressure dependence at 6 different gas pressures between 65 and 950 hPa. Further, we describe the
23 setup for this metrological validation, the challenges to overcome when assessing water vapor
24 measurements on a high accuracy level, as well as the comparison results. With this validation, SEALDH-II
25 is the first airborne, metrologically validated humidity transfer standard which links several scientific
26 airborne and laboratory measurement campaigns to the international metrological water vapor scale.

27
28
29 **1. Introduction**

30 Water vapor affects, like no other substance, nearly all atmospheric processes (Ludlam, 1980; Möller et al.,
31 2011; Ravishankara, 2012). Water vapor represents not only a large direct feedback to global warming when
32 forming clouds, but also plays a major role in atmospheric chemistry (Held and Soden, 2000; Houghton,
33 2009; Kiehl and Trenberth, 1997). Changes in the water distribution, as vapor or in condensed phases (e.g. in
34 clouds), have a large impact on the radiation balance of the atmosphere. This justifies that water vapor is
35 often mentioned as the most important greenhouse gas and one of the most important parameters in
36 climate research (Ludlam, 1980; Maycock et al., 2011). Water vapor measurements are often needed for
37 other in-situ atmospheric analyzers to correct for their water vapor cross-interference. The high (spatial and
38 temporal) variability of atmospheric water vapor, its large dynamic range (typically 3 – 40 000 ppmv), and

39 its broad spectroscopic fingerprint typically require complex multi-dimensional calibrations, in particular
40 for spectroscopic sensors. These calibrations often embrace the water vapor content of the gas flow to be
41 analyzed as one of the key calibration parameters even if the instrument (e.g. for CO₂), is not intended to
42 measure water vapor at all.

43 In particular for field weather stations, water vapor analyzers often are seen as part of the standard
44 instrumentation in atmospheric research. This seems reasonable due to several reasons: slow H₂O
45 concentration change over hours, the typical mid-range humidity levels (approx. above 5000 ppmv), no
46 significant gas pressure or temperature change, target accuracy often only in the on the order of 5-15%
47 relative deviation, and the absence of “non-typical atmospheric components” such as soot or hydrophobic
48 substances. Water vapor measurements under these conditions can be performed by a variety of different
49 devices (Wiederhold, 1997): Capacitive polymer sensors e.g. (Salasmaa and Kostamo, 1986) are frequently
50 deployed in low cost (field) applications. Small-scale produced, commercially available spectral absorption
51 devices e.g. (Petersen et al., 2010) are often used in research campaigns. Dew-point mirror hygrometers
52 (DPM) are known for their high accuracy. However, this is only true if they are regularly calibrated at high
53 accuracy (transfer-) standards in specialized hygrometry laboratories such as in metrology institutes
54 (Heinonen et al., 2012).

55 As soon as hygrometers have to be deployed in harsh environments (e.g. on airborne platforms), this
56 situation changes entirely: The ambient gas pressure (10 – 1000 hPa) and gas temperature (-90 – 40°C)
57 ranges are large and both values change rapidly, the required H₂O measurement range is set by the ambient
58 atmosphere (typically 3 – 40000 ppmv), mechanical stress and vibrations occur, and the sampled air
59 contains additional substances from condensed water (ice, droplets), particles, or even aircraft fuel vapor
60 (e.g. on ground). These and other impacts complicate reliable, accurate, long-term stable H₂O
61 measurements and briefly outline why water vapor measurements remain difficult in-situ measurements in
62 the field, even if they are nearly always needed in atmospheric science. Usually, the availability and
63 coverage of observations limit model validation studies in the first place but also the lack of sufficient
64 accuracy may have limited important scientific interpretations (Krämer et al., 2009; Peter et al., 2006; Scherer
65 et al., 2008; Sherwood et al., 2014).

66 Over the last decades, numerous hygrometers were developed and deployed on aircraft (Buck, 1985; Busen
67 and Buck, 1995; Cerni, 1994; Desjardins et al., 1989; Diskin et al., 2002; Durry et al., 2008; Ebert et al., 2000;
68 Gurlit et al., 2005; Hansford et al., 2006; Helten et al., 1998; Hunsmann et al., 2008; Karpechko et al., 2014;
69 Kley and Stone, 1978; May, 1998; Meyer et al., 2015; Ohtaki and Matsui, 1982; Roths and Busen, 1996;
70 Salasmaa and Kostamo, 1986; Schiff et al., 1994; Silver and Hovde, 1994a, 1994b; Thornberry et al., 2014;
71 Webster et al., 2004; Zöger et al., 1999a, 1999b) (non-exhaustive list), but those often show results which are
72 not sufficient for validation of atmospheric models in terms of the required absolute accuracy, precision,
73 temporal resolution, long-term stability, comparability, etc. These problems can be grouped into two major
74 categories: accuracy linked problems and time response linked problems. The latter is particularly
75 important for investigations in heterogeneous regions in the lower troposphere as well as for investigations
76 in clouds. In these regions, even two on average agreeing instruments with different response times yield

77 local, large, relative deviations on the order of up to 30% (Smit et al., 2014). In contrast to time response
78 studies, accuracy linked problems in flight are difficult to isolate since they are always covered by the
79 spatial variability (which leads to temporal variability for moving aircraft) of atmospheric H₂O distribution.
80 Comparing hygrometer in flight, such as, for example in (Rollins et al., 2014), does not facilitate a clear
81 accuracy assessment.

82 Therefore in 2007, an international intercomparison exercise named “AquaVIT” (Fahey et al., 2014) was
83 carried out to compare airborne hygrometers under quasi-static, laboratory-like conditions for upper
84 tropospheric and stratospheric humidity levels. AquaVIT (Fahey et al., 2014) encompassed 22 instruments
85 from 17 international research groups. The instruments were categorized in well-validated, often deployed
86 “core” instruments (APicT, FISH, FLASH, HWV, JLH, CFH) and “younger” non-core instruments.
87 AquaVIT revealed in the important 1 to 150 ppmv H₂O range, that -even under quasi-static conditions- the
88 deviation between the core instrument’s readings and their averaged group mean was on the order of ± 10
89 %. This result fits to the typical interpretation problems of flight data where instruments often deviate from
90 each other by up to 10%, which is not covered by the respective uncertainties of the individual instruments.
91 AquaVIT was a unique first step to document and improve the accuracy of airborne measurements in order
92 to make them more comparable. However, no instrument could claim after AquaVIT that its accuracy is
93 higher than any other AquaVIT instrument, since no “gold standard” was part of the campaign, i.e., a
94 metrological transfer standard (JCGM 2008, 2008; Joint Committee for Guides in Metrology (JCGM), 2009)
95 traced back to the SI units. There is no physical argument for the average being better than the measured
96 value of a single instrument. Instead, many arguments speak for systematic deviations of airborne
97 hygrometers: Most hygrometers have to be calibrated. Even for a perfect instrument, the accuracy issue is
98 represented by the calibration source and its gas handling system, which in this case leads to two major
99 concerns: First, one has to guarantee that the calibration source is accurate and stable under field conditions,
100 i.e., when using it before or after a flight on the ground. This can be challenging especially for the
101 transportation of the source with all its sensitive electronics/mechanics and for the deviating ambient
102 operation temperature from the ambient validation temperature (hangar vs. laboratory). Even more prone
103 to deviations are calibration sources installed inside the aircraft due to changing ambient conditions such as
104 cabin temperature, cabin pressure, orientation angle of instrument (important, if liquids are used for
105 heating or cooling). Secondly, the gas stream with a highly defined amount of water vapor has to be
106 conveyed into the instrument. Especially for water vapor, which is a strongly polar molecule, this gas
107 transport can become a critical step. Changing from high to low concentrations or even just changing the
108 gas pressure or pipe temperature can lead to signal creep due to slow adsorption and desorption processes,
109 which can take long to equilibrate. In metrology, this issue is solved by a long validation/calibration time
110 (hours up to weeks, depending on the H₂O concentration level), a generator without any connectors/fittings
111 (everything is welded) and piping made out of electro-polished, stainless steel to ensure that the
112 equilibrium is established before the actual calibration process is started. However, this calibration
113 approach is difficult to deploy and maintain for aircraft/field operations due to the strong atmospheric
114 variations in gas pressure and H₂O concentrations, which usually leads to a multi-dimensional calibration

115 pattern (H₂O concentration, gas pressure, sometimes also gas temperature) in a short amount of calibration
116 time (hours). Highly sensitive, frequently flown hygrometers like (Zöger et al., 1999a) are by their physical
117 principle, not as long-term stable as it would be necessary to take advantage of a long calibration session.
118 Besides the time issue to reach a H₂O equilibrium between source and instrument, most calibration
119 principles for water vapor are influenced by further issues. A prominent example is the saturation of air in
120 dilution/saturation based water vapor generators: gas temperature and pressure defines the saturation level
121 (described e.g. by Sonntag's Equation (Rollins et al., 2014)), however, it is well-known that e.g. 100.0%
122 saturation is not easily achievable. This might be one of the impact factors for a systematic offset during
123 calibrations in the field. The metrology community solves this for high humidity levels with large, multi-
124 step saturation chambers which decrease the temperature step-wise to force the water vapor to condense in
125 every following step. These few examples of typical field-related problems show, that there is a reasonable
126 doubt that deviations in field situations are norm-distributed. Hence, the mean during AquaVIT might be
127 biased, i.e. not the correct H₂O value.

128 The instruments by themselves might actually be more accurate than AquaVIT showed, but deficiencies of
129 the different calibration procedures (with their different calibration sources etc.) might mask this. To
130 summarize, AquaVIT documented a span of up to 20% relative deviation between the world's best airborne
131 hygrometers – but AquaVIT could not assess absolute deviations nor explain them, since a link to a
132 metrological H₂O primary standard (i.e., the definition of the international water vapor scale) was missing.
133 Therefore, we present in this paper the first comparison of an airborne hygrometer (SEALDH-II) with a
134 metrological standard for the atmospheric relevant gas pressure (65 – 950 hPa) and H₂O concentration
135 range (5 – 1200 ppmv). We will discuss the validation setup, procedure, and results. Based on this
136 validation, SEALDH-II is by definition the first airborne transfer standard for water vapor which links
137 laboratory and field campaigns directly to metrological standards.

138

139 **2. SEALDH-II**

140 **2.1. System description**

141 This paper focuses on the metrological accuracy validation of the **Selective Extractive Airborne Laser Diode**
142 **Hygrometer (SEALDH-II)**. SEALDH-II is the airborne successor of the proof-of-concept spectrometer
143 (SEALDH-I) study published in (Buchholz et al., 2014), which showed the possibility and the achievable
144 accuracy level for calibration-free dTDLAS hygrometry. The publication (Buchholz et al., 2014)
145 demonstrates this for the 600 ppmv to 20000 ppmv range at standard ambient pressure). The instruments
146 SEALDH-I, SEALDH-II and also HAI (Buchholz et al., 2017) are all three built with the design philosophy
147 that every single reported value of the instrument should have a “related boundary/operation condition
148 snap shot” allowing to exclude the possibility of any instrumental malfunction during the measurement.
149 SEALDH-II is from this perspective the most “holistic” approach (capturing much more boundary

150 condition data (Buchholz et al., 2016)), while HAI can serve as a multi-channel, multi-phase hygrometer for
151 a broader variety of scientific questions.

152 SEALDH-II integrates numerous different principles, concepts, modules, and novel parts, which contribute
153 to or enable the results shown in this paper. SEALDH-II's high internal complexity does not allow a full,
154 detailed discussion of the entire instrument in this paper; for more details the reader is referred to
155 (Buchholz et al., 2016). The following brief description covers the most important technical aspects of the
156 instrument from a user's point of view:

157 SEALDH-II is a compact (19" rack 4 U (=17.8 cm)) closed-path, absolute, directly Tunable Diode Laser
158 Absorption Spectroscopy (dTDLAS) hygrometer operating at 1.37 μm . With its compact dimensions and the
159 moderate weight (24 kg), it is well suited for space- and weight-limited airborne applications. The internal
160 optical measurement cell is a miniaturized White-type cell with an optical path length of 1.5 m (Kühnreich
161 et al., 2016; White, 1976). It is connected to the airplane's gas inlet via an internal gas handling system
162 comprising a temperature exchanger, multiple temperature sensors, a flow regulator, and two gas pressure
163 sensors.

164 Approximately 80 different instrument parameters are controlled, measured, or corrected by SEALDH-II at
165 any time to provide a holistic view on the spectrometer status. This extensive set of monitoring data ensures
166 reliable and well-characterized measurement data at any time. The knowledge about the instruments status
167 strongly facilitates metrological uncertainties calculations. SEALDH-II's calculated linear part of the
168 measurement uncertainty is 4.3%, with an additional offset uncertainty of ± 3 ppmv (further details in
169 (Buchholz et al., 2016)). The precision of SEALDH-II was determined via the Allan-variance approach and
170 yielded 0.19 ppmv (0.17 ppmv $\cdot\text{m}\cdot\text{Hz}^{-1/2}$) at 7 Hz repetition rate and an ideal precision of 0.056 ppmv (0.125
171 ppmv $\cdot\text{m}\cdot\text{Hz}^{-1/2}$) at 0.4 Hz. In general, SEALDH-II's time response is limited by the gas flow through the
172 White-type multi-pass measurement cell with a volume of 300 ml. With the assumption of a bulk flow of
173 7 SLM at 200 hPa through the cell, the gas exchange time is 0.5 seconds.

174 SEALDH-II's measurement range covers 3 – 40000 ppmv. The calculated mixture fraction offset uncertainty
175 of ± 3 ppmv defines the lower detection limit. This offset uncertainty by itself is entirely driven by the
176 capability of detecting and minimizing parasitic water vapor absorption. The concept, working principle,
177 and its limits are described in (Buchholz and Ebert, 2014). The upper limit of 40000 ppmv is defined by the
178 lowest internal instrument temperature, which has to always be higher than the dew point temperature to
179 avoid any internal condensation. From a spectroscopic perspective, SEALDH-II could handle
180 concentrations up to approx. 100000 ppmv before spectroscopic problems like saturation limit the accuracy
181 and increase the relative uncertainty beyond 4.3%.

182 **2.1. Calibration-free evaluation approach**

183 SEALDH-II's data treatment works differently from nearly all other published TDLAS spectrometers.
184 Typically, instruments are setup in a way that they measure the absorbance or a derivative measurand of
185 absorbance, and link it to the H₂O concentration. This correlation together with a few assumptions about
186 long-term stability, cross interference, gas temperature dependence, gas pressure dependence is enough to

187 calibrate a system (Muecke et al., 1994). Contrarily, a calibration-free approach requires a fully featured
188 physical model describing the absorption process entirely. The following description is a brief overview; for
189 more details see e.g. (Buchholz et al., 2014, 2016; Ebert and Wolfrum, 1994; Schulz et al., 2007).

190 In a very simplified way, our physical absorption model uses the *extended* Lambert-Beer equation (Equation
191 1) which describes the relationship between the initial light intensity $I_0(\lambda)$ before the absorption path
192 (typically being in the few mW-range) and the transmitted light intensity $I(\lambda)$.

193 Equation 1: $I(\lambda) = E(t) + I_0(\lambda) \cdot Tr(t) \cdot \exp[-S(T) \cdot g(\lambda - \lambda_0) \cdot N \cdot L]$

194 The parameter $S(T)$ describes the line strength of the selected molecular transition. In SEADLH-II's case, the
195 spectroscopic multi-line fit takes into account 19 transition lines in the vicinity of the target line at 1370 nm
196 (energy levels: 110 – 211, rotation-vibrational combination band). The other parameters are the line shape
197 function $g(\lambda - \lambda_0)$, the absorber number density N , the optical path length L and corrections for light-type
198 background radiation $E(t)$ and broadband transmission losses $Tr(t)$.

199 Equation 1 can be enhanced with the ideal gas law to calculate the H₂O volume mixing ratio c :

200 Equation 2:
$$c = - \frac{k_B \cdot T}{S(T) \cdot L \cdot p} \int \ln \left(\frac{I(\nu) - E(t)}{I_0(\nu) \cdot Tr(t)} \right) \frac{d\nu}{dt} dt$$

201 The additional parameters in Equation 2 are: constant entities like the Boltzmann constant k_B ; the optical
202 path length L ; molecular constants like the line strength $S(T)$ of the selected molecular transition; the
203 dynamic laser tuning coefficient $\frac{d\nu}{dt}$, which is a constant laser property; continuously measured entities such
204 as gas pressure (p), gas temperature (T) and photo detector signal of the transmitted light intensity $I(\nu)$ as
205 well as the initial light intensity $I_0(\nu)$, which is retrieve during the evaluation process from the transmitted
206 light intensity $I(\nu)$.

207 Equation 2 facilitates an evaluation of the measured spectra without any instrument calibration at any kind
208 of water vapor reference (Buchholz et al., 2014; Ebert and Wolfrum, 1994; Schulz et al., 2007) purely based
209 on first principles. Our concept of a fully calibration-free data evaluation approach (this excludes also any
210 referencing of the instrument to a water standard in order to correct for instrument drift, offsets,
211 temperature dependence, pressure dependence, etc.) is crucial for the assessment of the results described in
212 this publication. It should be noted that the term “calibration-free” is frequently used in different
213 communities with dissimilar meanings. We understand this term according to the following quote (JCGM
214 2008, 2008): “calibration (...) in a first step, establishes a relation between the measured values of a quantity
215 with measurement uncertainties provided by a measurement standard (...), in a second step, [calibration]
216 uses this information to establish a relation for obtaining a measurement result from an indication (of the
217 device to be calibrated)”. Calibration-free in this sense means, that SEALDH-II does not use any
218 information from “calibration-, comparison-, test-, adjustment-” runs with respect to a higher accuracy
219 “water vapor standard” to correct or improve any response function of the instrument. SEALDH-II uses as
220 described in (Buchholz et al., 2016) only spectroscopic parameters and the 80 supplementary parameters as
221 measurement input to calculate the final H₂O concentration. The fundamental difference between a

222 calibration approach and this stringent concept is that only effects which are part of our physical model are
223 taken into account for the final H₂O concentration calculation. All other effects like gas pressure or
224 temperature dependencies, which cannot be corrected with a well-defined physical explanation, remain in
225 our final results even if this has the consequence of slightly uncorrected results deviations. This strict
226 philosophy leads to measurements which are very reliable with respect to accuracy, precision and the
227 instrument's over-all performance. The down-side is a relatively computer-intensive, sophisticated
228 evaluation. As SEALDH-II stores all the raw spectra, one could – if needed for whatever reason – also
229 calibrate the instrument by referencing it to a high accuracy water vapor standard and transfer the better
230 accuracy e.g. of a metrological standard onto the instrument. Every calibration-free instrument can be
231 calibrated since pre-requirements for a calibration are just a subset of the requirements for a calibration-free
232 instrument. However, a calibration can only improve the accuracy for the relatively short time between two
233 calibration-cycles by adding all uncertainty contributions linked to the calibration itself to the system. This
234 is unpleasant or even intolerable for certain applications and backs our decision to develop a calibration-
235 free instrument to enable a first principles, long-term stable, maintenance-free and autonomous hygrometer
236 for field use e.g. at remote sites or aircraft deployments.

237 **3. SEALDH-II validation facility**

238 **3.1. Setup**

239 Figure 1 right shows the validation setup. As a well-defined and highly stable H₂O vapor source, we use a
240 commercial Thunder scientific model (TSM) 3900, similar to (Thunder-Scientific, 2016). This source
241 saturates pre-dried air at an elevated gas pressure in an internally ice covered chamber. The gas pressure in
242 the chamber and the chamber's wall temperature are precisely controlled and highly stable and thus define
243 the absolute water vapor concentration via the Sonntag equation (Sonntag, 1990). After passing through the
244 saturator, the gas expands to a pressure suitable for the subsequent hygrometer. The pressure difference
245 between the saturation chamber pressure and the subsequent step give this principle its name "two
246 pressure generator". The stable H₂O concentration range of the TSM is 1 – 1300 ppmv for these specific
247 deployment conditions. This generator provides a stable flow of approximately 4 – 5 SLM. Roughly 0.5 SLM
248 are distributed to a frost/dew point hygrometer, D/FPH, (MBW 373) (MBW Calibration Ltd., 2010).
249 SEALDH-II is fed with approx. 3.5 SLM, while 0.5 SLM are fed to an outlet. This setup ensures that the dew
250 point mirror hygrometer (DPH)¹ operates close to the ambient pressure, where its metrological primary
251 calibration is valid, and that the gas flow is sufficiently high in any part of the system to avoid recirculation
252 of air. The vacuum pump is used to vary the gas pressure in SEALDH-II's cell with a minimized feedback
253 on the flow through the D/FPH and the TSM. This significantly reduces the time for achieving a stable

¹ The used dew point mirror hygrometer can measure far below 0°C; therefore, it is a dew point mirror above > 0°C and a frost point mirror as soon as there is ice on the mirror surface. We will use both DPH and D/FPH abbreviations interchangeably.

254 equilibrium after any gas pressure change in SEALDH-II's chamber. SEALDH-II's internal electronic flow
255 regulator limits the mass flow at higher gas pressures and gradually opens towards lower pressures
256 (vacuum pumps usually convey a constant volume flow i.e., the mass flow is pressure dependent). We
257 termed this entire setup "traceable humidity generator", THG, and will name it as such throughout the text.

258 **3.1. Accuracy of THG**

259 The humidity of the gas flow is set by the TSM generator but the absolute H₂O values are traceably
260 determined with the dew point mirror hygrometer (D/FPH). The D/FPH, with its primary calibration, thus
261 guarantees the absolute accuracy in this setup. The D/FPH is not affected by the pressure changes in
262 SEALDH-II's measurement cell and operates at standard ambient gas pressure and gas temperature where
263 its calibration is most accurate. The D/FPH was calibrated (Figure 2) at the German national standard for
264 mid-range humidity (green, 600 – 8000 ppmv) as well as at the German national standard for low-range
265 humidity (blue, for lower values 0.1 – 500 ppmv). The two national standards work on different principles:
266 The two pressure principle (Buchholz et al., 2014) currently supplies the lower uncertainties (green, "±"-
267 values in Figure 2). Uncertainties are somewhat higher for the coulometric generator (Mackrodt, 2012) in
268 the lower humidity range (blue). The "Δ"-values in Figure 2 show the deviations between the readings of
269 the D/FPH and the "true" values of the national primary standards.

270 **4. SEALDH-II validation procedure**

271 **4.1. Mid-term multi-week permanent operation of SEALDH-II**

272 One part of the validation was a permanent operation of SEALDH-II over a time scale much longer than the
273 usual air or ground based scientific campaigns. In this paper, we present data from a permanent 23 day
274 long (550 operation hours) operation in automatic mode. Despite a very rigorous and extensive monitoring
275 of SEALDH-II's internal status, no malfunctions of SEALDH-II could be detected. One reason for this are
276 the extensive internal control and error handling mechanisms introduced in SEALDH-II, which are
277 mentioned above and described elsewhere (Buchholz et al., 2016). Figure 3 shows an overview of the entire
278 validation. The multi-week validation exercise comprises 15 different H₂O concentration levels between 2
279 and 1200 ppmv. At each concentration level, the gas pressure was varied in six steps (from 65 to 950 hPa)
280 over a range which is particularly interesting for instruments on airborne platforms operating from
281 troposphere to lower stratosphere where SEALDH-II's uncertainty (4.3% ± 3 ppmv) is suitable. Figure 3
282 (top) shows the comparison between SEALDH-II (black line) and the THG setup (red). Figure 3 (bottom)
283 shows the gas pressure (blue) and the gas temperature (green) in SEALDH-II measurement cell. The gas
284 temperature increase in the second week was caused by a failure of the laboratory air conditioner that led to
285 a higher room temperature and thus higher instrument temperature. Figure 4 shows the 200 hPa section of
286 the validation in Figure 3. To avoid any dynamic effects from time lags, hysteresis of the gas setup, or the
287 instruments themselves, every measurement at a given concentration/pressure combination lasted at least

288 60 min. The data from the THG (red) show that there is nearly no feedback of a gas pressure change in
289 SEALDH-II's measurement cell towards the D/FPH, respectively the entire THG. The bottom subplot in
290 Figure 4 shows the relative deviation between the THG and SEALDH-II. This deviation is correlated to the
291 absolute gas pressure level and can be explained by deficiencies of the Voigt lines shape used to fit
292 SEALDH-II's spectra (Buchholz et al., 2014, 2016). The Voigt profile, a convolution of Gaussian (for
293 temperature broadening) and Lorentzian (pressure broadening) profiles used for SEALDH-II's evaluation,
294 does not include effects such as Dicke Narrowing, which become significant at lower gas pressures.
295 Neglecting these effects cause systematic, but long-term stable and fully predictable deviations from the
296 reference value in the range from sub percent at atmospheric gas pressures to less than 5 % at the lowest gas
297 pressures described here. We have chosen not to implement any higher order line shape (HOLS) models as
298 the spectral reference data needed are not available at sufficient accuracy. Further, HOLS would force us to
299 increase the number of free fitting parameters, which would destabilize our fitting procedure, and lead to
300 reduced accuracy/reliability (i.e., higher uncertainty) as well as significantly increased computational
301 efforts. This is especially important for flight operation where temporal H₂O fluctuations (spatial
302 fluctuations result in temporal fluctuations for a moving device) occur with gradients up to 1000 ppmv/s.
303 These well understood, systematic pressure dependent deviations will be visible in each further result plot
304 of this paper. The impact and methods of compensation are already discussed in (Buchholz et al., 2014). The
305 interested reader is referred to this publication for a more detailed analysis and description.
306 SEALDH-II's primary target areas of operations are harsh field environments. Stability and predictability is
307 to be balanced with potential, extra levels of accuracy which might not be required or reliably achievable
308 for the intended application. Higher order line shape models are therefore deliberately traded for a stable,
309 reliable, and unified fitting process under all atmospheric conditions. This approach leads to systematic,
310 predictable deviations in the typical airborne accessible atmospheric gas pressure range (125 – 900 hPa) of
311 less than 3%. One has to compare these results for assessment to the non-systematic deviations of 20%
312 revealed during the mentioned AquaVIT comparison campaign (Fahey et al., 2014). Hence, for
313 field/airborne purposes, the 3% seems to be fully acceptable – especially in highly H₂O structured
314 environments.
315 This comparison with AquaVIT should just provide a frame to embed the 3%. The H₂O concentration range
316 of Aquavit (0 – 150 ppmv) versus this validation range (5 -1200 ppmv) and the instruments configuration at
317 AquaVIT (mainly (upper) stratospheric hygrometers) versus SEALDH-II as a wide range instrument (3 –
318 40000 ppmv) do not allow a direct comparison. Sadly, there is no other reliable (representative for the
319 community, externally reviewed, blind submission, etc.) comparison exercise such as AquaVIT for higher
320 concentration ranges.

321 **4.1. Assessment of SEALDH-II's mid-term accuracy: Dynamic effects**

322 Besides the pressure dependence discussed above, SEALDH-II's accuracy assessment is exacerbated by the
323 differences in the temporal behavior between the THG's dew/frost point mirror hygrometer (D/FPH) and
324 SEALDH-II: Figure 5 (left) shows an enlarged 45 min. long section of measured comparison data. SEALDH-

325 II (black) shows a fairly large water vapor variation compared to the THG (red). The precision of SEALDH-
326 II (see chapter 2) is 0.056 ppmv at 0.4 Hz (which was validated at a H₂O concentration of 600 ppmv
327 (Buchholz et al., 2016)) yielding a signal to noise ratio of 10700. Therefore, SEALDH-II can very precisely
328 detect variations in the H₂O concentration. Contrarily, the working principle of a D/FPH requires an
329 equilibrated ice/dew layer on the mirror. Caused by the inertial thermal adjustment process, the response
330 time of a dew/frost point mirror hygrometer has certain limitations due to this principle (the dew/frost
331 point temperature measurement is eventually used to calculate the final H₂O concentration), whereas the
332 optical measurement principle of SEALDH-II is only limited by the gas transport, i.e., the flow (exchange
333 rate) through the measurement cell. The effect of those different response times is clearly visible from 06:00
334 to 06:08 o'clock in Figure 5. The gas pressure of SEALDH-II's measurement cell (blue), which is correlated
335 to the gas pressure in the THG's ice chamber, shows an increase of 7 hPa – caused by the regulation cycle of
336 the THG's generator (internal saturation chamber gas pressure change). The response in the THG frost
337 point measurement (green, red) shows a significant time delay compared to SEALDH-II, which detects
338 changes approx. 20 seconds faster. This signal delay is also clearly visible between 06:32 to 06:40 o'clock,
339 where the water vapor variations detected by SEALDH-II are also visible in the smoothed signals of the
340 THG. Figure 5 right shows such a variation in detail (5 min). The delay between the THG and SEALDH-II is
341 here also approximately 20 seconds. If we assume that SEALDH-II measures (due to its high precision) the
342 true water vapor fluctuations, the relative deviation can be interpreted as overshooting and undershooting
343 of the D/FPH's controlling cycle, which is a commonly known response behavior of slow regulation
344 feedback loops to fast input signal changes. The different time responses lead to "artificial" noise in the
345 concentration differences between SEALDH-II and THG. Theoretically, one could characterize this behavior
346 and then try to correct/shift the data to minimize this artificial noise. However, a D/FPH is fundamentally
347 insufficient for a dynamic characterization of a fast response hygrometer such as SEALDH-II. Thus, the
348 better strategy is to keep the entire system as stable as possible and calculate mean values by using the
349 inherent assumption that under- and overshoots of the DPM affect the mean statically and equally. With
350 this assumption, the artificial noise can be seen in the first order as Gaussian distributed noise within each
351 pressure step (Figure 4) of at least 60 min. The error induced by this should be far smaller than the above
352 discussed uncertainties of the THG (and SEALDH-II).

353

354 **5. Results**

355 The results of this validation exercise are categorized in three sections according to the following conditions
356 in atmospheric regions: mid-tropospheric range: 1200 – 600 ppmv (Figure 6), upper tropospheric range: 600
357 – 20 ppmv (Figure 7), and lower stratospheric range: 20 – 5 ppmv (Figure 8). This categorization is also
358 justified by the relative influence of SEALDH-II's calculated offset uncertainty of ± 3 ppmv (Buchholz and
359 Ebert, 2014): At 1200 ppmv, its relative contribution of 0.25% is negligible compared to the 4.3% linear part
360 of the uncertainty of SEALDH-II. At 5 ppmv, the relative contribution of the offset uncertainty is 60% and

361 thus dominates the linear part of the uncertainty. Before assessing the following data, it should be
362 emphasized again that SEALDH-II's spectroscopic first-principles evaluation was designed to rely on
363 accurate spectral data instead of a calibration. SEALDH-II was never calibrated or referenced to any kind of
364 reference humidity generator or sensor.

365 **5.1. The 1200 – 600 ppmv range**

366 Figure 6 shows the summary of the pressure dependent validations in the 1200 – 600 ppmv range. Each of
367 the 48 data points represents the mean over one pressure measurement section of at least 60 min (see Figure
368 4). A cubic polynomial curve fitted to the 600 ppmv results (blue) serves as an internal quasi-reference to
369 connect with the following graphs. The 600 ppmv data (grey) are generated via a supplementary
370 comparison at a different generator: The German national primary mid-humidity generator (PHG). This
371 primary generator data at 600 ppmv indicate a deviation between PHG and THG of about 0.35 %, which is
372 compatible with the uncertainties of the THG (see chapter 3.1) and the PHG (0.4%) (Buchholz et al., 2014).
373 The PHG comparison data also allow a consistency check between the absolute values of (see Figure 2) the
374 PHG (calibration-free), the THG (DPM calibrated) and SEALDH-II (calibration-free).

375 **5.2. The 600 – 20 ppmv range**

376 In this range, the linear part of the uncertainty (4.3%) and the offset uncertainty (± 3 ppmv) have both a
377 significant contribution. Figure 7 shows a clear trend: The lower the concentration, the higher the deviation.
378 We believe this is being caused by SEALDH-II's offset variation and will be discussed in the 20 – 5 ppmv
379 range.

380 **5.3. The 20 – 5 ppmv range**

381 The results in this range (Figure 8) are dominated by the offset uncertainty. It is important to mention at this
382 point, that the ± 3 ppmv uncertainties are calculated based on assumptions, design innovations, and several
383 independent, synchronous measurements which are automatically done while the instrument is in
384 operation mode (see publication (Buchholz et al., 2016; Buchholz and Ebert, 2014)). Hence, the calculated
385 uncertainties resemble an upper uncertainty threshold; the real deviation could be lower than 3 ppmv. A
386 clear assessment is fairly difficult since at low concentrations (i.e., low optical densities) several other effects
387 occur together such as, e.g., optical interference effects like fringes caused by the very long coherence length
388 of the used laser. However, Figure 9 (left) allows a rough assessment of the offset instability. This plot
389 shows all the data below 200 ppmv, grouped by the gas pressure in the measurement cell. If one ignores the
390 65 hPa and 125 hPa measurements, which are clearly affected by higher order line shape effects (see above),
391 the other measurements fit fairly well in a ± 1 ppmv envelope function (grey). In other words, SEALDH-II's
392 combined offset "fluctuations" are below 1 ppmv H₂O. All validation measurements done with SEALDH-II
393 during the last years consistently demonstrated a small offset variability so that the observed offset error is
394 around 0.6 ppmv — i.e., only 20% of the calculated ± 3 ppmv.

395 5.4. General evaluation

396 Figure 9 presents a summary of all 90 analyzed concentration/pressure-pairs during the 23 days of
397 validation. The calculated uncertainties (linear 4.3% and offset ± 3 ppmv) of SEALDH-II are plotted in
398 purple. This uncertainty calculation doesn't include line shape deficiencies and is therefore only valid for a
399 pressure range where the Voigt profile can be used to represent all major broadening effects of absorption
400 lines (Dicke, 1953; Maddaloni et al., 2010). This is the case above 250 hPa. The results at 950, 750, 500,
401 250 hPa show that the maximum deviations, derived from these measurements, can be described by: linear
402 +2.5%, offset -0.6 ppmv.

403 To prevent further interpretations, it should be noted that this result doesn't change the statement about
404 SEALDH-II's uncertainties, since these are calculated and not based on any validation/calibration process.
405 This is a significantly different approach: The holistic control/overview is one of the most important and
406 essential differences between calibration-free instruments such as SEALDH-II and other classical
407 spectroscopic instruments which rely on sensor calibration. SEALDH-II can guarantee correctness of
408 measurement values within its uncertainties because any effect which causes deviations has to be included
409 in the evaluation model – otherwise it is not possible to correct for it.

410 As mentioned before, any calibration-free instrument can be calibrated too (see e.g. (Buchholz et al., 2013)).
411 However by doing so, one must accept to a certain extent loss of control over the system, especially in
412 environments which are different from the calibration environment. For example, if a calibration was used
413 to remove an instrumental offset, one has to ensure that this offset is long-term stable, which is usually
414 quite difficult, as - shown by the example of parasitic water offsets in fiber coupled diode laser hygrometers
415 (Buchholz and Ebert, 2014). Another option is to choose the recalibration frequency high enough; i.e.,
416 minimizing the drift amplitude by minimizing the time between two calibrations. This, however, reduces
417 the usable measurement time and leads to considerable investment of time and money into the calibration
418 process. For the case of SEALDH-II, a calibration of the pressure dependence – of course tempting and easy
419 to do – would directly “improve” SEALDH-II's laboratory overall performance level from $\pm 4.3\% \pm 3$ ppmv
420 to $\pm 0.35\% \pm 0.3$ ppmv. At first glance, this “accuracy” would then be an improvement by a factor of 55
421 compared to the mentioned results of AquaVIT (Fahey et al., 2014). However, it is extremely difficult – if
422 not impossible – to guarantee this performance and the validity of the calibration under harsh field
423 conditions; instead SEALDH-II would “suffer” from the same typical calibration associated problems in
424 stability and in predictability. Eventually, the calibration-free evaluation would define the trusted values
425 and the “improvement”, achieved by the calibration, would have to be used very carefully and might
426 disappear eventually.

427 6. Conclusion and Outlook

428 The SEALDH-II instrument; a novel, compact, airborne, calibration-free hygrometer which implements a
429 holistic, first-principles directly tuneable diode laser absorption spectroscopy (dTDLAS) approach was
430 stringently validated at a traceable water vapor generator at the German national metrology institute (PTB).

431 The pressure dependent validation covered a H₂O range from 5 to 1200 ppmv and a pressure range from
432 65 hPa to 950 hPa. In total, 90 different H₂O concentration/pressure levels were studied within 23 days of
433 permanent validation experiments. Compared to other comparisons of airborne hygrometers - such as those
434 studied in the non-metrological AquaVIT campaign (Fahey et al., 2014), where a selection of the best “core”
435 instruments still showed an accuracy scatter of at least $\pm 10\%$ without an absolute reference value - our
436 validation exercise used a traceable reference value derived from instruments directly linked to the
437 international dew-point scale for water vapor. This allowed a direct assessment of SEALDH-II’s absolute
438 performance with a relative accuracy level in the sub percent range. Under these conditions, SEALDH-II
439 showed an excellent absolute agreement within its uncertainties which are 4.3% of the measured value plus
440 an offset of ± 3 ppmv (valid at 1013 hPa). SEALDH-II showed at lower gas pressures - as expected - a stable,
441 systematic, pressure dependent offset to the traceable reference, which is caused by the line shape
442 deficiencies of the Voigt line shape: e.g. at 950 hPa, the systematic deviation of the calibration-free evaluated
443 results could be described by (linear +0.9%, offset -0.5 ppmv), while at 250 hPa the systematic deviations
444 could be described by (linear +2.5%, offset -0.6 ppmv). If we suppress this systematic pressure dependence,
445 the purely statistical deviation is described by linear scatter of $\pm 0.35\%$ and an offset uncertainty of
446 ± 0.3 ppmv.

447 Due to its extensive internal monitoring and correction infrastructure, SEALDH-II is very resilient against a
448 broad range of external disturbances and has an output signal temperature coefficient of only 0.026%/K,
449 which has already been validated earlier (Buchholz et al., 2016). Therefore, these results can be directly
450 transferred into harsh field environments. With this metrological, mid and upper atmosphere focused
451 validation presented here, we believe SEALDH-II to be the first directly deployable, metrologically
452 validated, airborne transfer standard for atmospheric water vapor. Having already been deployed in
453 several airborne and laboratory measurement campaigns, SEALDH-II thus directly links for the first time,
454 scientific campaign results to the international metrological water vapor scale.

455 ***Data availability***

456 *The underlying data for the results shown in this paper are raw spectra (time vs. photo current), which are compressed*
457 *to be compatible with the instruments data storage. In the compressed state the total amount is approximately 6GB of*
458 *binary data. Uncompressed data size is approx. 60 GB. We are happy to share these data on request.*

459

460 ***Author Contributions***

461 *Bernhard Buchholz and Volker Ebert conceived and designed the experiments. Bernhard Buchholz performed the*
462 *experiments; Bernhard Buchholz and Volker Ebert analyzed the data and wrote the paper.*

463

464 ***Conflicts of Interest***

465 *The authors declare no conflict of interest*

466

467 ***Acknowledgements:***

468 *Parts of this work were embedded in the EMPIR (European Metrology Program for Innovation and Research) projects*
469 *METEOMET- 1 and METEOMET-2. The authors want to thank Norbert Böse and Sonja Pratzler (PTB Germany)*
470 *for operating the German primary national water standard and the traceable humidity generator. Last but not least,*
471 *the authors thank James McSpirtt (Princeton University) for the various discussions about reliable sensor designs*
472 *and Mark Zondlo (Princeton University) for sharing his broad knowledge about atmospheric water vapor*
473 *measurements.*
474

475 **7. References**

- 476 Buchholz, B., Afchine, A., Klein, A., Schiller, C. and Krämer, M.: HAI , a new airborne, absolute, twin dual-
477 channel, multi-phase TDLAS-hygrometer: background, design, setup, and first flight data, *Atmos. Meas.*
478 *Tech.*, 5194, <http://dx.doi.org/10.5194/amt-10-35-2017>, 2017.
- 479 Buchholz, B., Böse, N. and Ebert, V.: Absolute validation of a diode laser hygrometer via intercomparison
480 with the German national primary water vapor standard, *Applied Physics B*, 116(4), 883–899,
481 <http://dx.doi.org/10.1007/s00340-014-5775-4>, 2014.
- 482 Buchholz, B. and Ebert, V.: Offsets in fiber-coupled diode laser hygrometers caused by parasitic absorption
483 effects and their prevention, *Measurement Science and Technology*, 25(7), 75501,
484 <http://dx.doi.org/10.1088/0957-0233/25/7/075501>, 2014.
- 485 Buchholz, B., Kallweit, S. and Ebert, V.: SEALDH-II—An Autonomous, Holistically Controlled, First
486 Principles TDLAS Hygrometer for Field and Airborne Applications: Design–Setup–Accuracy/Stability
487 Stress Test, *Sensors*, 17(1), 68, <http://dx.doi.org/10.3390/s17010068>, 2016.
- 488 Buchholz, B., Kühnreich, B., Smit, H. G. J. and Ebert, V.: Validation of an extractive, airborne, compact TDL
489 spectrometer for atmospheric humidity sensing by blind intercomparison, *Applied Physics B*, 110(2), 249–
490 262, <http://dx.doi.org/10.1007/s00340-012-5143-1>, 2013.
- 491 Buck, A.: The Lyman-alpha absorption hygrometer, in *Moisture and Humidity Symposium Washington*,
492 DC, Research Triangle Park, NC, pp. 411–436., 1985.
- 493 Busen, R. and Buck, A. L.: A High-Performance Hygrometer for Aircraft Use: Description, Installation, and
494 Flight Data, *Journal of Atmospheric and Oceanic Technology*, 12, 73–84, [http://dx.doi.org/10.1175/1520-0426\(1995\)012<0073:AHPHFA>2.0.CO;2](http://dx.doi.org/10.1175/1520-0426(1995)012<0073:AHPHFA>2.0.CO;2), 1995.
- 496 Cerni, T. A.: An Infrared Hygrometer for Atmospheric Research and Routine Monitoring, *Journal of*
497 *Atmospheric and Oceanic Technology*, 11, 445–462, [http://dx.doi.org/10.1175/1520-0426\(1994\)011<0445:AIHFAR>2.0.CO;2](http://dx.doi.org/10.1175/1520-0426(1994)011<0445:AIHFAR>2.0.CO;2), 1994.
- 499 Desjardins, R., MacPherson, J., Schuepp, P. and Karanja, F.: An evaluation of aircraft flux measurements of
500 CO₂, water vapor and sensible heat, *Boundary-Layer Meteorology*, 47(1), 55–69,
501 <http://dx.doi.org/10.1007/BF00122322>, 1989.
- 502 Dicke, R.: The effect of collisions upon the Doppler width of spectral lines, *Physical Review*, 89(2), 472–473,
503 <http://dx.doi.org/10.1103/PhysRev.89.472>, 1953.
- 504 Diskin, G. S., Podolske, J. R., Sachse, G. W. and Slate, T. A.: Open-path airborne tunable diode laser
505 hygrometer, in *Proc. SPIE 4817, Diode Lasers and Applications in Atmospheric Sensing*, vol. 4817, pp. 196–
506 204., 2002.
- 507 Durry, G., Amarouche, N., Joly, L. and Liu, X.: Laser diode spectroscopy of H₂O at 2.63 μm for atmospheric
508 applications, *Applied Physics B*, 90(3–4), 573–580, <http://dx.doi.org/10.1007/s00340-007-2884-3>, 2008.
- 509 Ebert, V., Fernholz, T. and Pitz, H.: In-situ monitoring of water vapour and gas temperature in a coal fired
510 power-plant using near-infrared diode lasers, in *Laser Applications to Chemical and Environmental*
511 *Analysis*, pp. 4–6, Optical Society of America. [online] Available from:
512 <http://www.opticsinfobase.org/abstract.cfm?id=142068> (Accessed 15 February 2012), 2000.
- 513 Ebert, V. and Wolfrum, J.: Absorption spectroscopy, in *OPTICAL MEASUREMENTS-Techniques and*
514 *Applications*, ed. F. Mayinger, pp. 273–312, Springer., 1994.
- 515 Fahey, D. W., Saathoff, H., Schiller, C., Ebert, V., Peter, T., Amarouche, N., Avallone, L. M., Bauer, R.,
516 Christensen, L. E., Durry, G., Dyroff, C., Herman, R., Hunsmann, S., Khaykin, S., Mackrodt, P., Smith, J. B.,
517 Spelten, N., Troy, R. F., Wagner, S. and Wienhold, F. G.: The AquaVIT-1 intercomparison of atmospheric
518 water vapor measurement techniques, *Atmospheric Measurement Techniques*, 7, 3159–3251,
519 <http://dx.doi.org/10.5194/amtd-7-3159-2014>, 2014.
- 520 Gurlit, W., Zimmermann, R., Giesemann, C., Fernholz, T., Ebert, V., Wolfrum, J., Platt, U. U. and Burrows, J.

521 P.: Lightweight diode laser spectrometer “ CHILD ” for balloon- borne measurements of water vapor and
522 methane, *Applied Optics*, 44(1), 91–102, <http://dx.doi.org/10.1364/AO.44.000091>, 2005.

523 Hansford, G. M., Freshwater, R. A., Eden, L., Turnbull, K. F. V., Hadaway, D. E., Ostanin, V. P. and Jones, R.
524 L.: Lightweight dew-/frost-point hygrometer based on a surface-acoustic-wave sensor for balloon-borne
525 atmospheric water vapor profile sounding, *Review of scientific instruments*, 77, 014502–014502,
526 <http://dx.doi.org/10.1063/1.2140275>, 2006.

527 Heinonen, M., Anagnostou, M., Bell, S., Stevens, M., Benyon, R., Bergerud, R. A., Bojkovski, J., Bosma, R.,
528 Nielsen, J., Böse, N., Cromwell, P., Kartal Dogan, A., Aytakin, S., Uytun, A., Fernicola, V., Flakiewicz, K.,
529 Blanquart, B., Hudoklin, D., Jacobson, P., Kentved, A., Lóio, I., Mamontov, G., Masarykova, A., Mitter, H.,
530 Mnguni, R., Otych, J., Steiner, A., Szilágyi Zsófia, N. and Zvizdic, D.: Investigation of the equivalence of
531 national dew-point temperature realizations in the -50 °C to +20 °C range, *International Journal of*
532 *Thermophysics*, 33(8–9), 1422–1437, <http://dx.doi.org/10.1007/s10765-011-0950-x>, 2012.

533 Held, I. and Soden, B.: Water vapor feedback and global warming, *Annual review of energy and the*
534 *environment*, 25(1), 441–475, <http://dx.doi.org/10.1146/annurev.energy.25.1.441>, 2000.

535 Helten, M., Smit, H. G. J., Sträter, W., Kley, D., Nedelec, P., Zöger, M. and Busen, R.: Calibration and
536 performance of automatic compact instrumentation for the measurement of relative humidity from
537 passenger aircraft, *Journal of Geophysical Research: Atmospheres*, 103(D19), 25643–25652,
538 <http://dx.doi.org/10.1029/98JD00536>, 1998.

539 Houghton, J.: *Global warming: The complete briefing*, Cambridge University Press. [online] Available from:
540 <http://britastro.org/jbaa/pdf/114-6shanklin.pdf> (Accessed 14 May 2014), 2009.

541 Hunsmann, S., Wunderle, K., Wagner, S., Rascher, U., Schurr, U. and Ebert, V.: Absolute, high resolution
542 water transpiration rate measurements on single plant leaves via tunable diode laser absorption
543 spectroscopy (TDLAS) at 1.37 μm , *Applied Physics B*, 92(3), 393–401, [http://dx.doi.org/10.1007/s00340-008-](http://dx.doi.org/10.1007/s00340-008-3095-2)
544 [3095-2](http://dx.doi.org/10.1007/s00340-008-3095-2), 2008.

545 JCGM 2008: JCGM 200 : 2008 International vocabulary of metrology – Basic and general concepts and
546 associated terms (VIM) *Vocabulaire international de métrologie – Concepts fondamentaux et généraux et*
547 *termes associés (VIM)*, International Organization for Standardization, 3(Vim), 104,
548 [http://dx.doi.org/10.1016/0263-2241\(85\)90006-5](http://dx.doi.org/10.1016/0263-2241(85)90006-5), 2008.

549 Joint Committee for Guides in Metrology (JCGM): Evaluation of measurement data - An introduction to the
550 “Guide to the expression of uncertainty in measurement” and related documents, BIPM: Bureau
551 International des Poids et Mesures, www.bipm.org, 2009.

552 Karpechko, A. Y., Perlwitz, J. and Manzini, E.: *Journal of Geophysical Research : Atmospheres*, , 1–16,
553 <http://dx.doi.org/10.1002/2013JD021350>, 2014.

554 Kiehl, J. T. and Trenberth, K. E.: Earth’s Annual Global Mean Energy Budget, *Bulletin of the American*
555 *Meteorological Society*, 78(2), 197–208, [http://dx.doi.org/10.1175/1520-](http://dx.doi.org/10.1175/1520-0477(1997)078<0197:EAGMEB>2.0.CO;2)
556 [0477\(1997\)078<0197:EAGMEB>2.0.CO;2](http://dx.doi.org/10.1175/1520-0477(1997)078<0197:EAGMEB>2.0.CO;2), 1997.

557 Kley, D. and Stone, E.: Measurement of water vapor in the stratosphere by photodissociation with Ly α
558 (1216 Å) light, *Review of Scientific Instruments*, 49(6), 691, <http://dx.doi.org/10.1063/1.1135596>, 1978.

559 Krämer, M., Schiller, C., Afchine, A., Bauer, R., Gensch, I., Mangold, A., Schlicht, S., Spelten, N., Sitnikov,
560 N., Borrmann, S., Reus, M. de and Spichtinger, P.: Ice supersaturations and cirrus cloud crystal numbers,
561 *Atmospheric and Oceanic Optics*, 9, 3505–3522, <http://dx.doi.org/10.5194/acp-9-3505-2009>, 2009.

562 Kühnreich, B., Höh, M., Wagner, S. and Ebert, V.: Direct single-mode fibre-coupled miniature White cell for
563 laser absorption spectroscopy, *Review of Scientific Instruments*, 87(2), 0–8,
564 <http://dx.doi.org/10.1063/1.4941748>, 2016.

565 Ludlam, F.: *Clouds and storms: The behavior and effect of water in the atmosphere*. [online] Available
566 from: <http://agris.fao.org/agris-search/search.do?recordID=US8025686> (Accessed 24 May 2014), 1980.

567 Mackrodt, P.: A New Attempt on a Coulometric Trace Humidity Generator, *International Journal of*
568 *Thermophysics*, 33(8–9), 1520–1535, <http://dx.doi.org/10.1007/s10765-012-1348-0>, 2012.

569 Maddaloni, P., Malara, P. and Natale, P. De: Simulation of Dicke-narrowed molecular spectra recorded by
570 off-axis high-finesse optical cavities, *Molecular Physics*, 108(6), 749–755,
571 <http://dx.doi.org/10.1080/00268971003601571>, 2010.

572 May, R. D.: Open-path, near-infrared tunable diode laser spectrometer for atmospheric measurements of
573 H₂O, *Journal of Geophysical Research*, 103(D15), 19161–19172, <http://dx.doi.org/10.1029/98JD01678>, 1998.

574 Maycock, A. C., Shine, K. P. and Joshi, M. M.: The temperature response to stratospheric water vapour
575 changes, *Quarterly Journal of the Royal Meteorological Society*, 137, 1070–1082,
576 <http://dx.doi.org/10.1002/qj.822>, 2011.

577 MBW Calibration Ltd.: MBW 373HX, 2010.

578 Meyer, J., Rolf, C., Schiller, C., Rohs, S., Spelten, N., Afchine, A., Zöger, M., Sitnikov, N., Thornberry, T. D.,
579 Rollins, A. W., Bozoki, Z., Tatrai, D., Ebert, V., Kühnreich, B., Mackrodt, P., Möhler, O., Saathoff, H.,
580 Rosenlof, K. H. and Krämer, M.: Two decades of water vapor measurements with the FISH fluorescence
581 hygrometer: A review, *Atmospheric Chemistry and Physics*, 15(14), 8521–8538,
582 <http://dx.doi.org/10.5194/acp-15-8521-2015>, 2015.

583 Möller, D., Feichter, J. and Herrmann, H.: Von Wolken, Nebel und Niederschlag, in *Chemie über den*
584 *Wolken... und darunter*, edited by R. Zellner, pp. 236–240, WILEY-VCH Verlag GmbH & Co. KGaA,
585 Weinheim., 2011.

586 Muecke, R. J., Scheumann, B., Slemr, F. and Werle, P. W.: Calibration procedures for tunable diode laser
587 spectrometers, *Proc. SPIE 2112, Tunable Diode Laser Spectroscopy, Lidar, and DIAL Techniques for*
588 *Environmental and Industrial Measurement*, 2112, 87–98, <http://dx.doi.org/10.1117/12.177289>, 1994.

589 Ohtaki, E. and Matsui, T.: Infrared device for simultaneous measurement of fluctuations of atmospheric
590 carbon dioxide and water vapor, *Boundary-Layer Meteorology*, 24(1), 109–119,
591 <http://dx.doi.org/10.1007/BF00121803>, 1982.

592 Peter, T., Marcolli, C., Spichtinger, P., Corti, T., Baker, M. B. and Koop, T.: When dry air is too humid,
593 *Science*, 314(5804), 1399–1402, <http://dx.doi.org/10.1126/science.1135199>, 2006.

594 Petersen, R., Cnonce, L., Feltz, W., Olson, E. and Helms, D.: WVSS-II moisture observations: A tool for
595 validating and monitoring satellite moisture data, *EUMETSAT Meteorological Satellite Conference*, 22, 67–
596 77 [online] Available from:
597 http://www.eumetsat.int/Home/Main/AboutEUMETSAT/Publications/ConferenceandWorkshopProceedings/2010/groups/cps/documents/document/pdf_conf_p57_s1_03_petersen_v.pdf (Accessed 20 February 2017),
598 2010.

600 Ravishankara, A. R.: Water Vapor in the Lower Stratosphere, *Science*, 337(6096), 809–810,
601 <http://dx.doi.org/10.1126/science.1227004>, 2012.

602 Rollins, A., Thornberry, T., Gao, R. S., Smith, J. B., Sayres, D. S., Sargent, M. R., Schiller, C., Krämer, M.,
603 Spelten, N., Hurst, D. F., Jordan, A. F., Hall, E. G., Vömel, H., Diskin, G. S., Podolske, J. R., Christensen, L.
604 E., Rosenlof, K. H., Jensen, E. J. and Fahey, D. W.: Evaluation of UT/LS hygrometer accuracy by
605 intercomparison during the NASA MACPEX mission, *Journal of Geophysical Research: Atmospheres*, 119,
606 <http://dx.doi.org/10.1002/2013JD020817>, 2014.

607 Roths, J. and Busen, R.: Development of a laser in situ airborne hygrometer (LISAH) (feasibility study),
608 *Infrared physics & technology*, 37(1), 33–38, [http://dx.doi.org/10.1016/1350-4495\(95\)00103-4](http://dx.doi.org/10.1016/1350-4495(95)00103-4), 1996.

609 Salasmaa, E. and Kostamo, P.: HUMICAP® thin film humidity sensor, in *Advanced Agricultural*
610 *Instrumentation Series E: Applied Sciences*, edited by W. G. Gensler, pp. 135–147, Kluwer., 1986.

611 Scherer, M., Vömel, H., Fueglistaler, S., Oltmans, S. J. and Staehelin, J.: Trends and variability of midlatitude
612 stratospheric water vapour deduced from the re-evaluated Boulder balloon series and HALOE,
613 *Atmospheric Chemistry and Physics*, 8, 1391–1402, <http://dx.doi.org/10.5194/acp-8-1391-2008>, 2008.

614 Schiff, H. I., Mackay, G. I. and Bechara, J.: The use of tunable diode laser absorption spectroscopy for
615 atmospheric measurements, *Research on Chemical Intermediates*, 20(3), 525–556,
616 <http://dx.doi.org/10.1163/156856794X00441>, 1994.

617 Schulz, C., Dreizler, A., Ebert, V. and Wolfrum, J.: Combustion Diagnostics, in Handbook of Experimental
618 Fluid Mechanics, edited by C. Tropea, A. L. Yarin, and J. F. Foss, pp. 1241–1316, Springer Berlin Heidelberg,
619 Heidelberg, 2007.

620 Sherwood, S., Bony, S. and Dufresne, J.: Spread in model climate sensitivity traced to atmospheric
621 convective mixing, *Nature*, 505(7481), 37–42, <http://dx.doi.org/10.1038/nature12829>, 2014.

622 Silver, J. A. and Hovde, D. C.: Near-infrared diode laser airborne hygrometer, *Review of scientific*
623 *instruments*, 65(5), 1691–1694, <http://dx.doi.org/10.1063/1.1144861>, 1994a.

624 Silver, J. and Hovde, D.: Near-infrared diode laser airborne hygrometer, *Review of scientific instruments*,
625 65, 5, 1691–1694 [online] Available from: http://ieeexplore.ieee.org/xpls/abs_all.jsp?arnumber=4991817
626 (Accessed 25 November 2013b), 1994.

627 Smit, H. G. J., Rolf, C., Kraemer, M., Petzold, A., Spelten, N., Neis, P., Maser, R., Buchholz, B., Ebert, V. and
628 Tatrai, D.: Development and Evaluation of Novel and Compact Hygrometer for Airborne Research
629 (DENCHAR): In-Flight Performance During AIRTOSS-I / II Research Aircraft Campaigns, *Geophysical*
630 *Research Abstracts*, 16(EGU2014-9420), 2014.

631 Sonntag, D.: Important new Values of the Physical Constants of 1968, Vapour Pressure Formulations based
632 on the ITS-90, and Psychrometer Formulae, *Meteorologische Zeitschrift*, 40(5), 340–344, 1990.

633 Thornberry, T. D., Rollins, A. W., Gao, R. S., Watts, L. A., Ciciora, S. J., McLaughlin, R. J. and Fahey, D. W.:
634 A two-channel, tunable diode laser-based hygrometer for measurement of water vapor and cirrus cloud ice
635 water content in the upper troposphere and lower stratosphere, *Atmospheric Measurement Techniques*
636 *Discussions*, 7(8), 8271–8309, <http://dx.doi.org/10.5194/amtd-7-8271-2014>, 2014.

637 Thunder-Scientific: Model 2500 Two-Pressure Humidity Generator, [online] Available from:
638 www.thunderscientific.com (Accessed 12 May 2016), 2016.

639 Webster, C., Flesch, G., Mansour, K., Haberle, R. and Bauman, J.: Mars laser hygrometer, *Applied optics*,
640 43(22), 4436–4445, <http://dx.doi.org/10.1364/AO.43.004436>, 2004.

641 White, J.: Very long optical paths in air, *Journal of the Optical Society of America* (1917-1983), 66(5), 411–
642 416, <http://dx.doi.org/10.1364/JOSA.66.000411>, 1976.

643 Wiederhold, P. R.: Water Vapor Measurement. Methods and Instrumentation, Har/Dskt., CRC Press., 1997.

644 Zöger, M., Afchine, A., Eicke, N., Gerhards, M.-T., Klein, E., McKenna, D. S., Mörschel, U., Schmidt, U., Tan,
645 V., Tuitjer, F., Woyke, T. and Schiller, C.: Fast in situ stratospheric hygrometers: A new family of balloon-
646 borne and airborne Lyman photofragment fluorescence hygrometers, *Journal of Geophysical Research*,
647 104(D1), 1807–1816, <http://dx.doi.org/10.1029/1998JD100025>, 1999a.

648 Zöger, M., Engel, A., McKenna, D. S., Schiller, C., Schmidt, U. and Woyke, T.: Balloon-borne in situ
649 measurements of stratospheric H₂O, CH₄ and H₂ at midlatitudes, *Journal of Geophysical Research*,
650 104(D1), 1817–1825, <http://dx.doi.org/10.1029/1998JD100024>, 1999b.

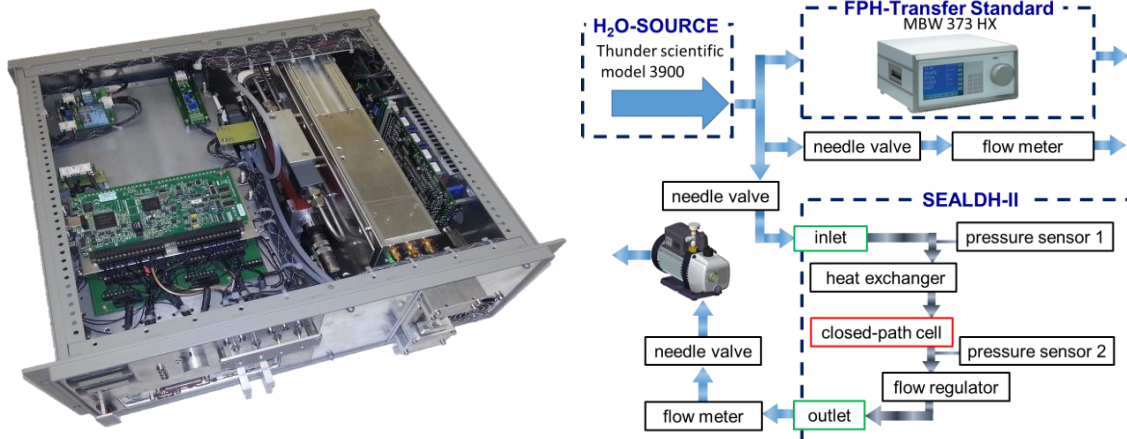
651

652

653 **Figures:**

654

655

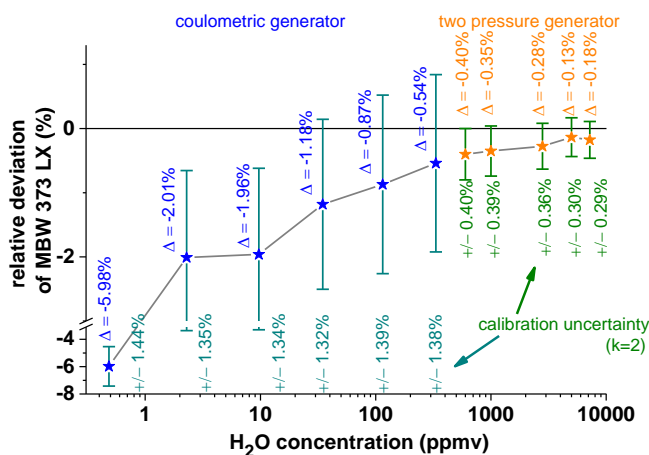


656 Figure 1: Left: Photo of SEALDH-II, the Selective Extractive Airborne Laser Diode Hygrometer (dimension 19" 4 U).
 657 Right: Setup for the metrological absolute accuracy validation. The combination of a H₂O source together with a
 658 traceable dew point hygrometer, DPM, is used as a transfer standard – a traceable humidity generator (THG).
 659

660

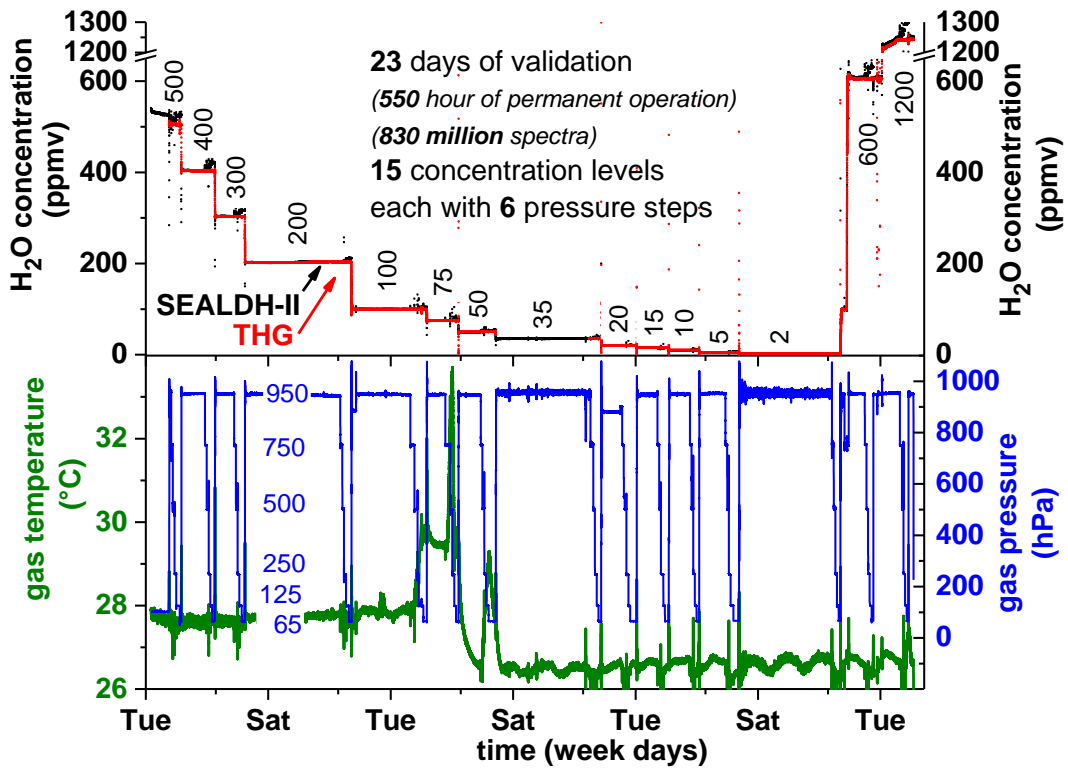
661

662



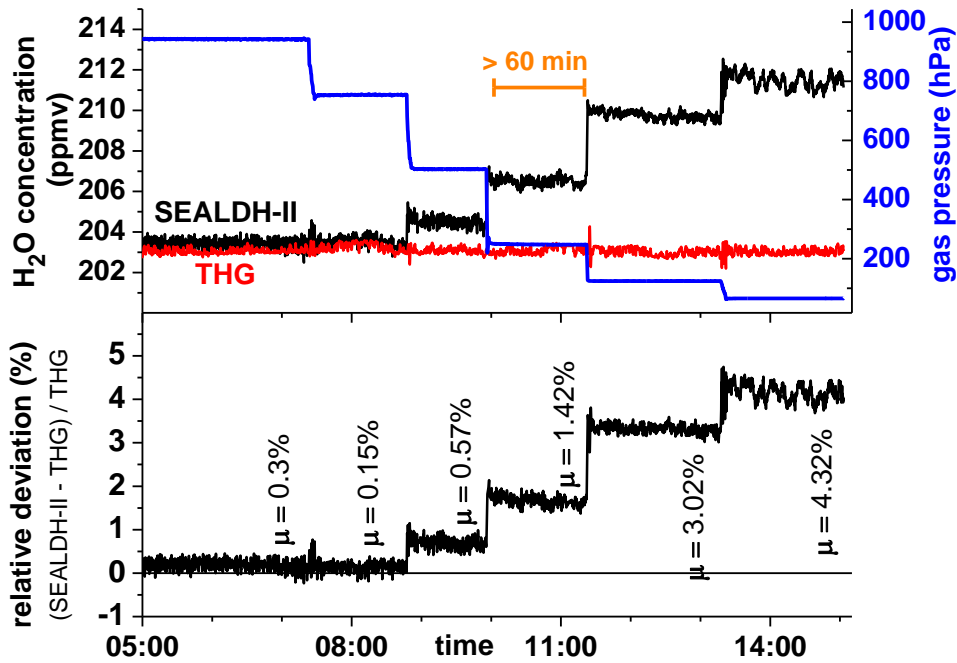
663 Figure 2: Calibration of the DPM (dew/frost point mirror hygrometer, MBW 373 LX, which is used as part of the THG)
 664 at the national primary water vapor standards of Germany. The standard for the higher H₂O concentration range
 665 (orange) is a “two pressure generator” (Buchholz et al., 2014); for the lower concentration range (blue) a “coulometric
 666 generator” (Mackrodt, 2012) is used as a reference. The deviations between reference and DPM are labelled with “Δ”.
 667 The uncertainties of every individual calibration point are stated as green numbers below every single measurement
 668 point.
 669

670
671
672



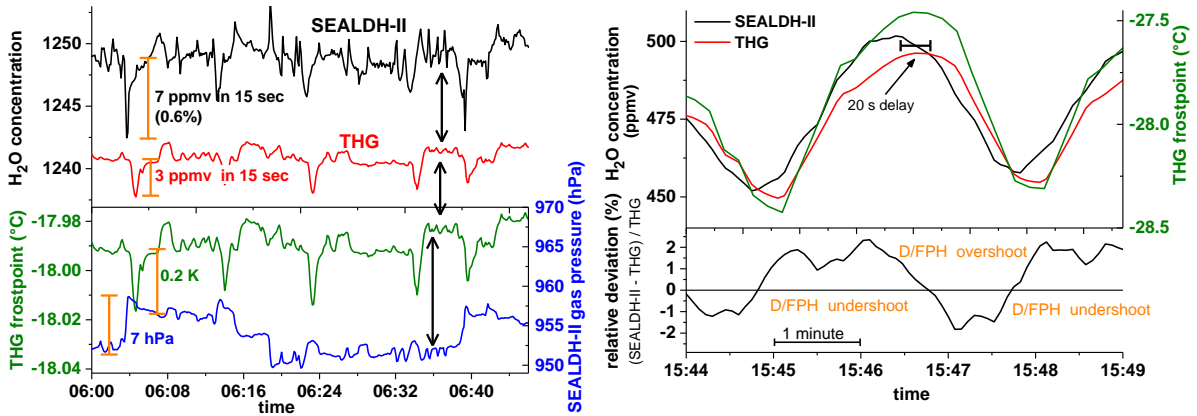
673
674 Figure 3: Overview showing all data recorded over 23 days of validation experiments. Measurements of the traceable
675 humidity generator (THG) are shown in red, SEALDH-II data in black, gas pressure and gas temperature in SEALDH-
676 II's measurement cell are shown in blue and green. Note: SEALDH-II operated the entire time without any
677 malfunctions; the THG didn't save data in the 35 ppmv section; the temperature increase during the 75 ppmv section
678 was caused by a defect of the air conditioning in the laboratory.

679
680
681
682



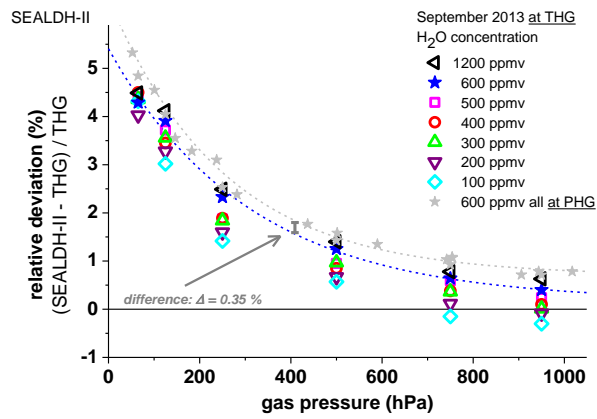
683
 684 Figure 4: Detailed plot of the validation at 200 ppmv with six gas pressure steps from 50 to 950 hPa. Each individual
 685 pressure level was maintained for at least 60 minutes in order to avoid any dynamic or hysteresis effects and to
 686 facilitate clear accuracy assessments. The μ -values define the averaged relative deviation on every gas pressure level.

687
 688
 689



690
 691 Figure 5: Short term H₂O fluctuations in the generated water vapor flow measured by SEALDH-II and the dew/frost
 692 point mirror hygrometer (D/FPH) of the traceable humidity generator (THG). The different dynamic characteristics of
 693 SEALDH-II (fast response time) and THG (quite slow response) lead in a direct comparison to artificial noise.
 694 Oscillating behaviors like in the right figure occur when the THG is not equilibrated. We did not use such data
 695 segments for the accuracy assessments.

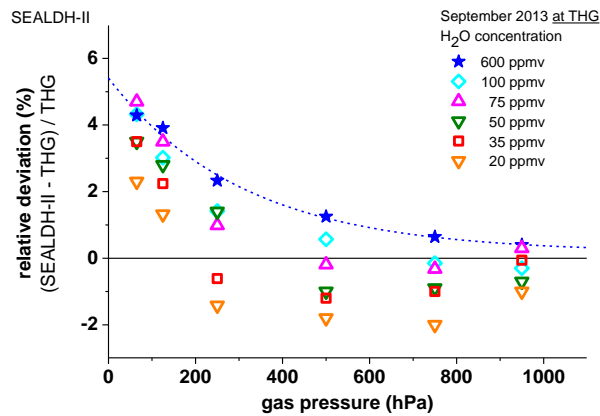
696
 697
 698
 699



700
 701 Figure 6: Gas pressure dependent comparison between SEALDH-II and THG over a H₂O concentration range from 600
 702 to 1200 ppmv and a pressure range from 50 to 950 hPa. The 600 ppmv values (in grey) are measured directly at the
 703 national primary humidity generator (PHG) of Germany; all other H₂O concentration values are measured at and
 704 compared to the traceable humidity generator (THG). All SEALDH-II spectra were evaluated with a calibration-free
 705 first principles evaluation based on absolute spectral parameters. No initial or repetitive calibration of SEALDH-II with
 706 respect to any “water reference” source was used.

707

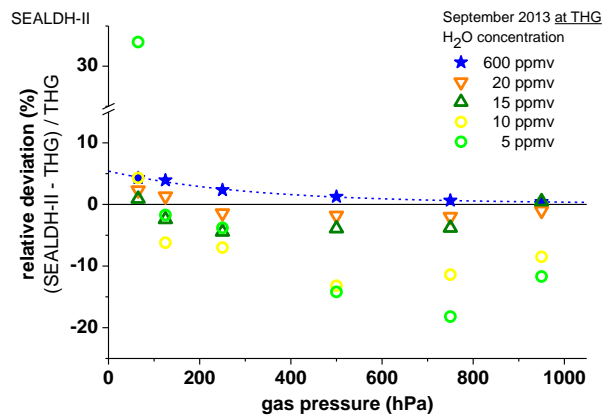
708



709
 710 Figure 7: Comparison results as in Figure 6 but for the 200 – 600 ppmv range.

711

712



713

714 Figure 8: Comparison results as in Figure 6 and Figure 7 but for the 5 – 20 ppmv range. All spectra are determined with
 715 a calibration-free first principles evaluation concept. The major contribution to the higher fluctuations at lower
 716 concentrations is the accuracy of the offset determination (details see text).

717

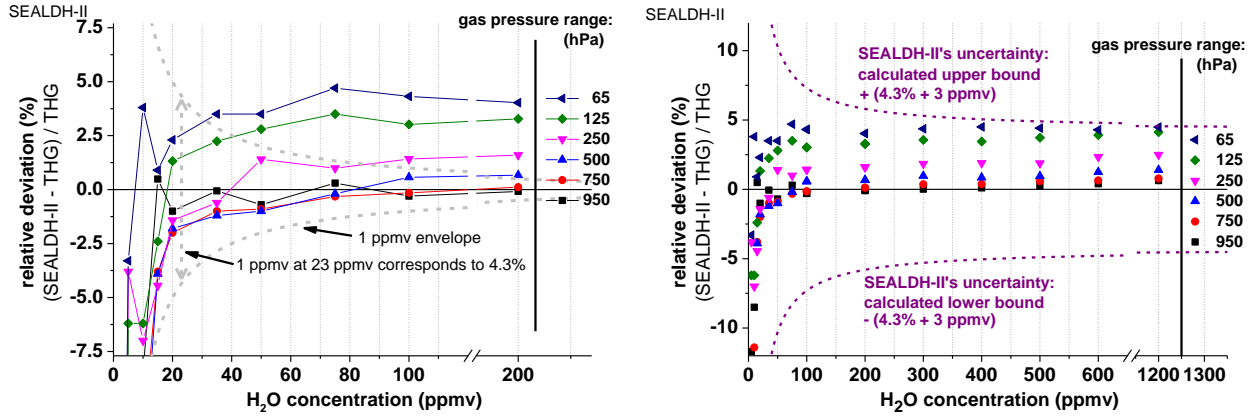


Figure 9: Direct comparison of SEALDH-II versus THG for H₂O concentrations between 5 and 200 ppmv and gas pressures from 65 to 950 hPa. Both figures show the relative deviations between SEALDH-II and THG grouped and color-coded by gas-pressure. Left plot: relative deviations of SEALDH-II versus THG below 200 ppmv; the grey line indicates the computed relative effect in SEALDH-II's performance caused by ± 1 ppmv offset fluctuation. This line facilitates a visual comparison between an offset impact and the 4.3% linear part of the uncertainty of SEALDH-II. Right plot: relative deviations for all measured data in the same concentration range. Also shown is SEALDH-II's total uncertainty of 4.3% \pm 3 ppmv (calculated for 1013 hPa) as a dashed line.

718

719

720